

INCORPORATING THE HIGHER HARMONICS IN VIV FATIGUE PREDICTIONS

Vikas Jhingran

Department of Mechanical and Ocean
Engineering
Massachusetts Institute of Technology

Prof. J. Kim Vandiver

Department of Mechanical and Ocean
Engineering
Massachusetts Institute of Technology

ABSTRACT

Vortex-Induced Vibrations (VIV) are an important source of fatigue damage for risers in the Oil and Gas industry. Results from recent VIV experiments by Vandiver et al. [1] indicate significant dynamic strain energy at not only the Strouhal frequency, but also its harmonics. In certain regions of the pipe, these higher harmonics accounted for more than half of the measured RMS strain and increased fatigue damage by a factor exceeding twenty. However, the state-of-the-art in VIV prediction only accounts for the vibrations at the Strouhal frequency.

Preliminary results from a second set of experiments, described in this paper, confirm the importance of the higher harmonics in fatigue life estimates of pipes. Further, the authors formulate an approach to incorporate the higher harmonics in VIV related fatigue design. Finally, the authors identify the estimation of the higher harmonics, in both location and magnitude, as an important area of ongoing research, the results of which will be required to implement this proposed method.

INTRODUCTION

Vortex-Induced Vibrations (VIV) response has been discussed in the offshore engineering literature for over twenty five years and the higher harmonics have also been noticed since the early experiments [2, 3]. It is common knowledge that the in-line frequency is twice the Strouhal frequency. The third and fifth harmonics were noticed in accelerometer measurements described in the late 1980s [3], but were not considered to be of significant concern when making fatigue life estimates. This was because the response at the frequency of the third and fifth harmonics was quite small in these early, low mode number experiments on flexible cylinders in uniform and sheared flows.

Recent experiments [1], where higher modes were excited, have shown that the higher harmonics can be very important for VIV related fatigue damage. These higher harmonics were found to cause large amplifications, sometimes greater than twenty, in fatigue damage in certain regions of a pipe

undergoing VIV. However, the state-of-the-art in VIV prediction does not account for the higher harmonics. In fact, a hydrodynamic explanation for the existence of the third harmonic was only recently presented by Williamson et al. [4]. New data, from the second Gulf Stream experiments, sometimes shows the occurrence of a strong fifth harmonic.

These higher harmonics present an interesting challenge for an engineer designing risers. They have been shown to have important fatigue-related consequences in certain regions of the pipe. On the other hand, no method or guidance is available to include their effects in design. In fact, the procedures used to predict VIV related fatigue damage were not developed with the higher harmonics in mind. It is therefore important that we revisit these formulations and modify them in light of the findings from the Gulf Stream experiments.

EXPERIMENT DESCRIPTION

The second Gulf Stream experiment is the third of a series of field experiments, conducted by Deepstar and MIT, to study VIV response of flexible pipes at high mode numbers. The first experiment was carried out at a US Navy test facility on Lake Seneca in upstate New York in the summer of 2004. The Lake Seneca tests focused on the effect of VIV at high mode numbers for a pipe in uniform flow. The second experiment was conducted in the Gulf Stream near Miami. The first of the Gulf Stream tests, conducted in the fall of 2004, focused on a long pipe in sheared flow. The second Gulf Stream test, the focus of this paper, was conducted in the fall of 2006. All three tests were part of a larger testing program developed by DEEPSTAR, a joint industry technology development project, aimed at improving the ability to model and mitigate VIV.

The goals of the overall test program were to understand the different aspects of the dynamics of a pipe undergoing VIV at high mode numbers. These aspects included VIV suppression with strakes, drag coefficients of bare and straked pipes, in-line and cross-flow VIV, and damping factors. The importance of the higher harmonics to fatigue, as reported by Vandiver et al. [1], was found in data collected in these experiments. This

paper outlines a methodology to include these higher harmonic frequencies in the fatigue damage calculations for a flexible pipe.

The Second Gulf Stream Experiment

The Gulf Stream tests were conducted on the Research Vessel F. G. Walton Smith from the University of Miami using a glass fiber composite pipe 500.4 ft. long and 1.43 inches in diameter. The pipe was spooled on a drum that was mounted on the aft portion of the ship. The pipe was lowered directly from the drum into the water. A railroad wheel weighing 805 lbs (dry weight, 725 lbs in water), was attached to the bottom of the pipe to provide tension, as was done in the Lake Seneca experiment.

The top end of the pipe was attached to the stern of the boat with a universal joint to provide a pinned boundary condition. The boat steered on various headings relative to the Gulf Stream so as to produce a large variety of sheared currents, varying from nearly uniform to highly sheared in speed and direction. Eight optical fibers were embedded in the outer layers of the composite pipe. Each fiber contained thirty five strain gauges, which use the principle of Bragg diffraction to measure strain with a resolution of approximately 1 micro-strain. Two fibers were located in each of the four quadrants of the pipe, as seen in Figure 1.

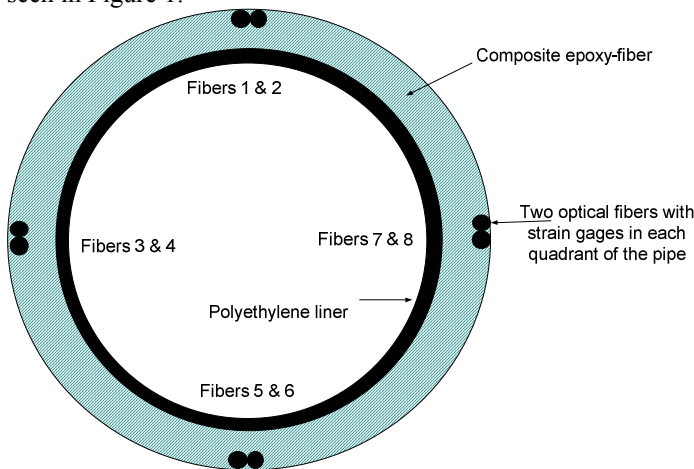


Figure 1 - Cross-Section of the Pipe from the Gulf Stream Test

Each fiber had a strain gauge spacing of 14 ft.. Each quadrant pair of fibers was positioned so that the strain gauges in one fiber were offset from the gauges in the other fiber by 7 ft., as shown in Figure 3. The fiber optic strain gauge system was provided by Insensys, Ltd. in the UK. The fibers were embedded in the pipe during manufacture by Fiberspar at their fabrication facility in Houston.

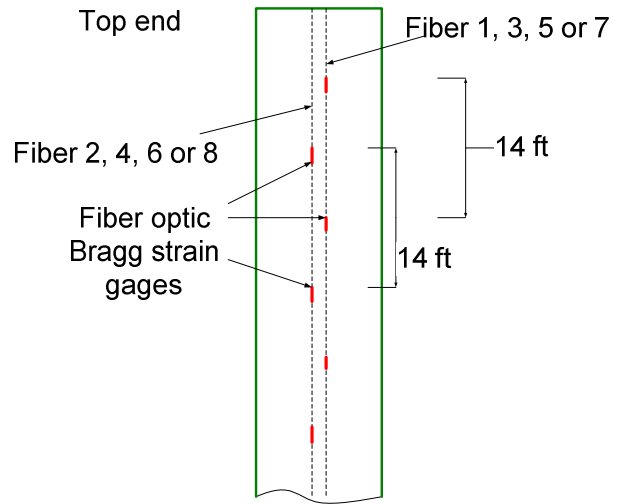


Figure 2 - Side View of the Pipe from the Gulf Stream Test

The pipe was made of fiberglass with an HDPE liner. The pipe properties are found in Table 1.

Table 1 –Gulf Stream Pipe Properties

Inner Diameter	0.98 in (0.02489 m)
Outer Diameter	1.43 in (0.03632 m)
Optical Fiber Diameter	1.37 in (0.035 m)
EI	2.14e5 lb.in ² (613 Nm ²)
EA	1.33e6 lb/ in ² (9.21e9 N/m ²)
Weight in Seawater	0.133 lb/ft (flooded in seawater) (1.942 N/m)
Weight in air, wo/trapped water	0.511 lb/ft (7.46 N/m)
Weight in air, w/trapped water	0.846 lb/ft (12.35 N/m)
Effective Tension (at bottom end)	725 lbs submg. Bottom weight (3225)
Material	Fiberglass
Length	500.4 ft (152.4) U-Joint to U-Joint

An Acoustic Doppler Current profiler (ADCP) recorded the current velocity and direction along the length of the pipe. On the R/V F. G. Walton Smith, there are two ADCPs. Each ADCP uses a different frequency to obtain different currents at different depths. The broadband (600 kHz) ADCP records the current at greater resolution and accuracy to a depth of about 60 ft., whereas the narrowband (75 kHz) ADCP records the current up to about 1500 ft. During the Gulf Stream testing both ADCPs were used to gather data.

Additional instrumentation included a tilt meter to measure the inclination at the top of the pipe, a load cell to measure the tension in the pipe, two mechanical current meters to measure current at the top and the bottom of the pipe and a pressure gauge to measure the lift of the pipe bottom during tow.

Wave induced vessel motion during the Gulf Stream test added low frequency components to the strain time series. An elliptical filter with a 1.5 Hz cut-off was used to remove this vessel motion from the data without interfering with the VIV frequencies. The filtering was done such that no phase shift was applied to the data.

ANALYSIS OF RESPONSE DATA

Experiments done in the field, like the Gulf Stream and Lake Seneca tests, cannot achieve laboratory like control over environment conditions. Vessel motions and variability in boat speed, for example, can cause the incident velocity on the pipe to vary during an experiment. Further, manufacturing expenses and time schedules can prohibit the achievement of the desired level of perfection in the experimental equipment. In the Gulf Stream experiments, for example, the optical fibers were twisted during manufacturing of the pipe such that the circumferential location of a particular fiber changed along the length of the pipe. This resulted in no fiber being perfectly aligned with either cross-flow or in-line directions for the entire length of the pipe.

Fortunately, these issues could be addressed using data post-processing techniques. In particular, steady state regions were identified to avoid frequent shifts in the fundamental VIV frequency caused due to changes in the incident current velocity on the pipe. Moreover, strain signals from two orthogonal sensors were combined to recover the total cross-flow and in-line strain components.

Establishing steady state regions

Figure 3 (a) presents data from a bare pipe test (Test – 20061023203818) performed during the second Gulf Stream experiment. It shows time-frequency plots, called scalograms, at three locations on the pipe. The frequency range in these plots is chosen to show the Strouhal frequency, called the fundamental VIV frequency or $1x$ frequency in this paper. Figure 3 (b) shows the mean normal incident current¹ on the pipe during the test. The scalograms were calculated at sensor locations 232.5 ft (sensor 33), 302.5 ft (sensor 43) and 372.5 ft (sensor 53) measured axially from the top of the pipe. Their positions on the pipe are shown by dots in Figure 3 (b).

The scalograms indicate that the fundamental frequency of VIV was not constant for the duration of the test. They suggest that the frequency reached a steady state value only in the last sixty seconds of the test. Since the motion of the pipe is mainly governed by the fundamental VIV frequency, we can make the assumption that steady state conditions are achieved when this frequency is steady with time. Experimental data from these steady-state regions can be used to make comparisons with results from predictive programs, like Shear7, which assume steady state conditions in their analysis.

In this steady state region, the fundamental frequency of vibration and all its harmonics are narrow banded, almost single frequency responses. Figure 4 shows the strain Power Spectral Density (PSD) for the steady state duration of the test. These PSDs, shown for orthogonal quadrants Q4 and Q1, correspond to the same sensor locations as the scalograms. The PSD peaks are labeled as $1x$, $2x$, etc. where the “ x ” should be interpreted as “times the fundamental VIV frequency of vibration.” This terminology will be used for the rest of the paper.

¹ The current profile had to be corrected for incidence angle of the pipe.

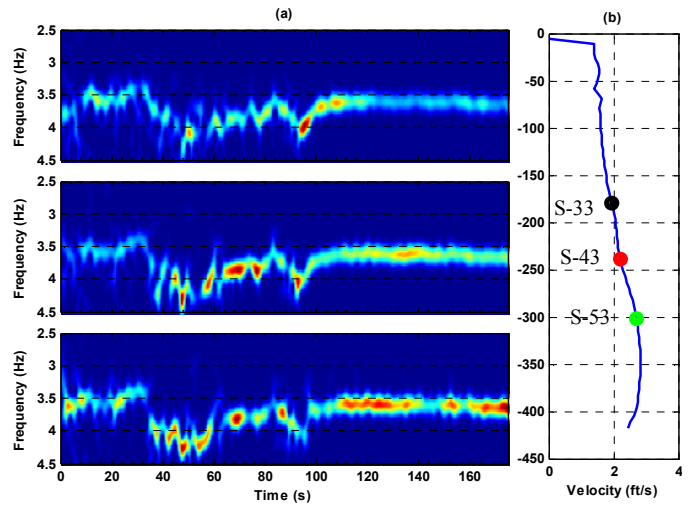


Figure 3 (a) - Time-Frequency plots for test 20061023203818 show that steady state conditions are achieved only in the last 60 seconds. The plots were obtained using the Morlet Wavelet analysis. (b) The normal incident current profile with locations where the wavelet transforms shown in (a) were performed.

As expected, the PSDs show energy not only at the fundamental frequency of vibration but also at its harmonics. Of these, the third harmonic and the fifth harmonic are of particular interest.

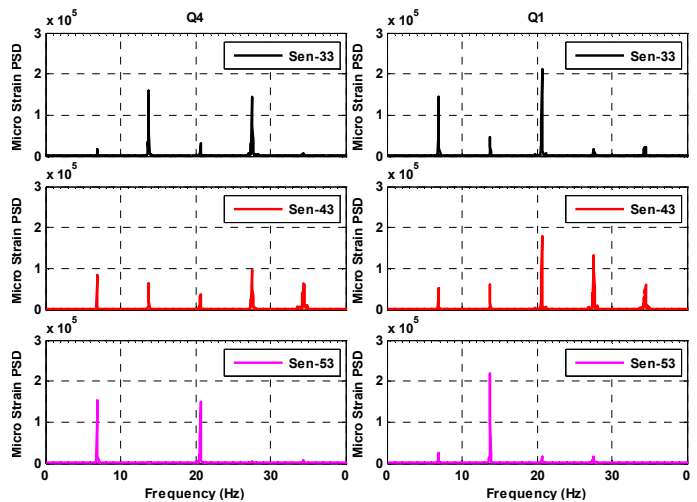


Figure 4 –Strain PSDs, shown for Q4 and Q1, in the steady state region are almost single frequency responses. Each PSD was calculated using the Welch method with 60 seconds of data, a 40 second window length and 95% overlap.

Calculating total cross-flow and in-line strain

Previous research has shown that the odd harmonics are associated with the cross-flow direction while the even harmonics are seen in the in-line direction. Indeed, when a sensor in the Gulf Stream experiment was exactly aligned with the cross-flow direction, the odd harmonics dominated in the PSD. However, the twist in the fibers along the pipe resulted in

sensor orientations which were neither in-line nor cross-flow. This explains why the PSDs in Figure 4 contain energy in both the odd and even harmonic frequencies.

In order to make comparisons with predictive programs like Shear7, which predict the 1x response in the cross-flow direction, the response measured by a pair of orthogonal sensors should be transformed to a new co-ordinate system aligned with the cross-flow and in-line directions. However, this was not always possible because data from some fibers was not perfectly synchronous during the experiments. This made it impossible to rotate the strain data into new co-ordinate systems because orthogonal strain measurements were not available at the same time instant. It was more feasible to calculate total energy at a particular frequency using PSDs from two orthogonal fibers.

The strain data from each quadrant was filtered to isolate the signal corresponding to each of the harmonics. Spectra for 1x components from orthogonal quadrants were then summed to produce a spectrum that represents the total energy in the 1x component. This was done for each of the harmonics. Finally, the spectra corresponding to the odd harmonics, i.e. first, third and fifth, were summed to produce the spectral representation of the total energy in the cross-flow direction. Figure 5 shows the total cross-flow and in-line energy for locations corresponding to sensors 33, 43 and 53.

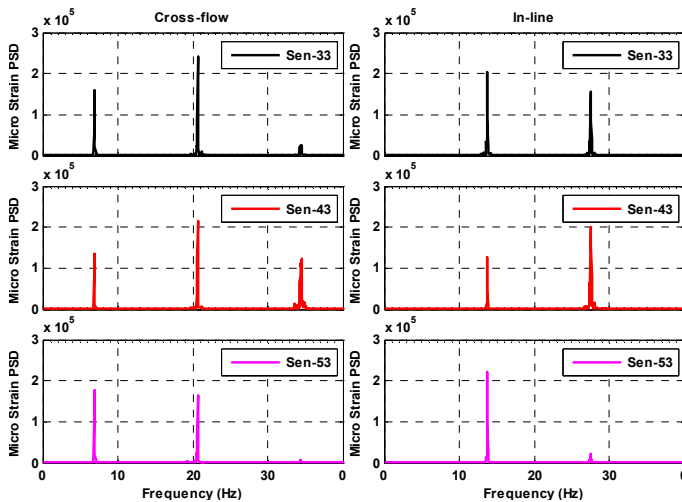


Figure 5 - PSDs of strain from orthogonal quadrants processed to isolate the energy in the odd harmonics to form the total cross-flow strain spectrum and the energy in the even harmonics to form the total in-line strain spectrum.

CONTRIBUTIONS OF THE HIGHER HARMONICS

Comparisons with Shear7

Once steady-state regions within individual experiments have been identified, results from these regions can be used to benchmark and evaluate the performance of the state-of-the-art in VIV prediction. Further, the contributions of the higher harmonics to strain and fatigue, assuming material of pipe to be steel, can be investigated. As VIV prediction programs, like

Shear7, only predict the 1x response, results from the above analysis will indicate the importance of incorporating the fatigue effects of the higher harmonics in predictive programs.

For the current profile shown in Figure 3(b) and a model with physical properties corresponding to the pipe used in the second Gulf Stream experiments, Shear7-V4.5² was used to make VIV response predictions. Figure 6 compares the total measured RMS strain in the cross-flow direction to that predicted by Shear7-V4.5. Also shown is the contribution of the 1x component to the total cross-flow strain. The results indicate that Shear7 predicts the 1x response well but does not account for the increase in RMS strain due to the higher harmonics. This is to be expected.

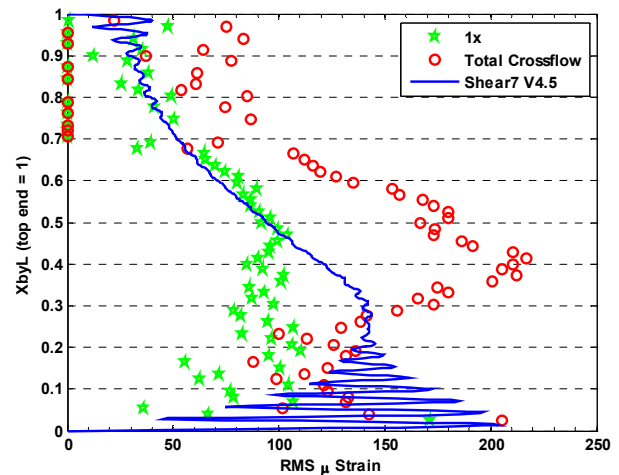


Figure 6 – Measured and predicted first harmonic RMS strain and measured RMS total cross-flow strain. Predicted strain from Shear7 v4.5, using CLtype=2, Single mode bandwidth = 0.4 and 8 timeshare modes with equal probability of occurrence.

This result brings forward two separate issues. First, it is encouraging to see that Shear7 accurately predicts the 1x strain component. Second, the contribution of the higher harmonics can be more than fifty percent of the total strain response in certain regions of the pipe. This increase in strain resulting from the higher harmonics can be particularly important when calculating fatigue damage due to VIV.

It should be pointed out that the Shear7 strain response in Figure 6 shows oscillatory behavior near the bottom boundary. This is due to a standing wave generated by the pinned boundary condition. This results in the maximum strain

² Shear7-V4.5 introduces the concept of timesharing of frequencies to VIV prediction. Pipe natural frequencies that are likely to be excited due to fluid flow, n in number, are assumed to occur independently in time for a fraction of the total duration based on their probability of occurrence, $p_a(i)$,

such that $\sum_{i=1}^n p_a(i) = 1$. The total fatigue damage is the sum of the fatigue damages due to each frequency multiplied with its probability of occurrence i.e.

$$D = \sum_{i=1}^n D_i \cdot p_a(i)$$

occurring close to the boundary. The standing wave pattern at the boundary is also observed in the measured 1x strain.

Fatigue prediction implications

Fatigue damage is proportional to (stress)^m, where m is the slope of the S-N curve and is usually between 3 and 4. As stress is proportional to strain, the increase in the RMS strain due to the higher harmonics, as seen in Figure 6, has a significant impact on the fatigue damage of the pipe. Assuming an API X' S-N curve and the Young's Modulus of Steel (Es) as 200x10⁶ MPa, Figure 7 compares the fatigue damage predicted from Shear7 to that calculated from the measured data (using the Dirlik method explained later in the paper) for the same case shown in Figure 6. If the Shear7 predictions in Figure 7 were used in design, the maximum predicted fatigue damage would occur in the standing wave at the boundary. SHEAR7 would not have predicted the location of the measured peak damage rate correctly, because of the contributions of the 3x and 5x components closer to the middle of the pipe.

Figure 8 shows the total damage rate, calculated from measured strain, along the pipe, normalized by the maximum Shear7V4.5 predicted damage on the pipe (Total damage/max(Shear7V.5 damage)). The location of the maximum predicted damage by Shear7V4.5 is near the boundary, as shown in Figure 7. The maximum damage rate implied from the data exceeds the maximum predicted by Shear7 by a factor of 3. This occurs at the location where the 3x and 5x components are largest. Although the actual damage rate is greater than the maximum predicted by a factor of 3, this is within the factor of safety normally used in the industry and could be a possible reason that failures in actual practice have not been observed.

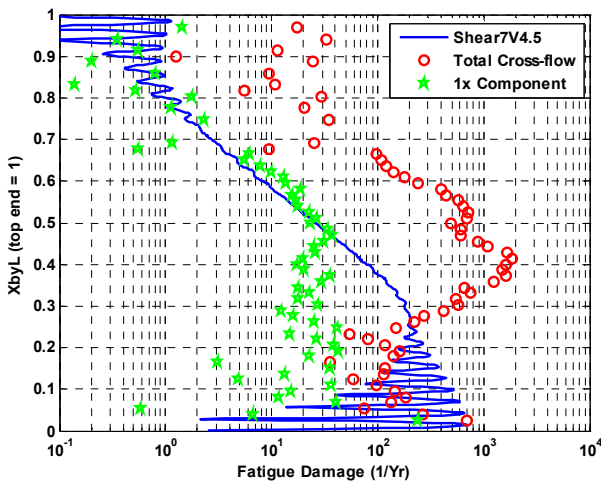


Figure 7 - Comparison of fatigue damage predicted by Shear7V4.5 to that calculated from measured data using the Dirlik method. Young's modulus for steel and API-X' S-N curve were used.

However, fatigue results presented as above may understate the significance of the higher harmonic contributions to fatigue. It is more realistic to examine the region of maximum stress due to the higher harmonics, and compute the ratio of the total

damage rate to the maximum 1x damage rate in the same region. The result is shown in Figure 9.

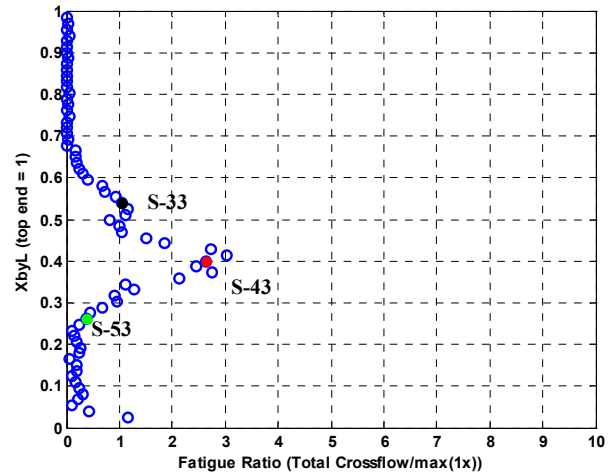


Figure 8 – The ratio of the total cross-flow damage to the maximum damage reported by Shear7-V4.5 anywhere on the pipe. The ratio at sensors 33, 43 and 53 are shown by dots.

FATIGUE FORMULATIONS

The offshore Oil and Gas industry primarily uses the S-N curve in conjunction with Miner's rule to estimate fatigue damage [5][6]. This method uses the stress range Probability Distribution Function (PDF) to compute the number of expected cycles at a particular frequency in unit time. The damage due to each frequency can then be calculated using experimentally determined S-N curves. Finally, the total fatigue damage is assumed to be the sum of fatigue damage due to each frequency.

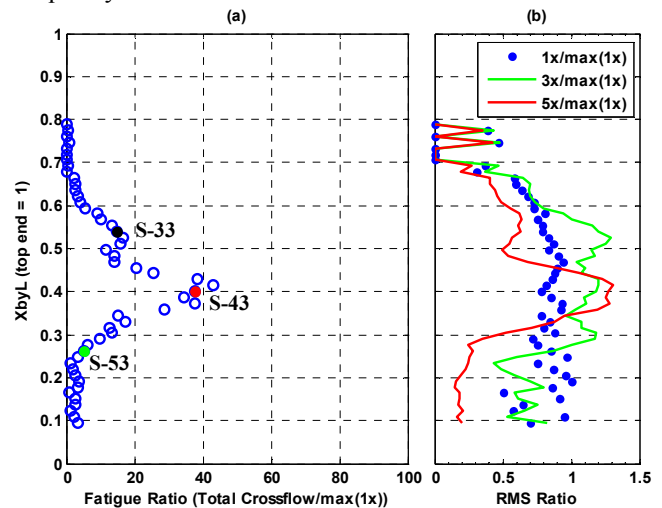


Figure 9 – 9a) The ratio of the total damage rate to the maximum 1x damage rate in the same region, which occurs at x/L=0.2. 9b) Individual 1x, 3x, and 5x damage rates normalized by the maximum 1x at x/L=0.2.

Figure 9a shows that the ratio of the total cross-flow VIV damage to the damage due the 1x component can be as high as 40 (the ratio at sensors 33, 43 and 53 are shown by dots).

Clearly, inaccuracies in the estimation of the stress range PDF can lead to significant error in the prediction of fatigue life of a structure. Historically, VIV stress time histories have been assumed to be a Gaussian narrow banded process, with energy only around the Strouhal frequency. This assumption allows the stress range PDF, $p_r(\sigma_r)$, to be represented by a Rayleigh probability distribution. The fatigue damage then is calculated using experimentally determined S-N curves.

It is instructive to go through the main steps of fatigue calculations. Fatigue damage accumulates over time due to stress range cycles acting over certain lengths of time. For a pipe undergoing VIV for T seconds, the total number, N, of expected stress cycles is

$$N = \frac{T}{T_z} ; T_z = \text{zero-crossing period}$$

The total number of stress cycles, N, is distributed into cycles at each stress range, n_r , based on the stress range PDF.

$$n_r = \frac{Tp_r(\sigma_r)\delta\sigma_r}{T_z} \quad (1.1)$$

The S-N curve method (where A and m are experimentally determined material constants) then gives us the damage caused by these n cycles with stress range σ_r as

$$\delta D = \frac{n}{A\sigma_r^{-m}} = \frac{Tp_r(\sigma_r)\delta\sigma_r}{T_z A\sigma_r^{-m}} \quad (1.2)$$

$$\text{Total Damage} = \int \delta D \quad (1.3)$$

$$D = \frac{T}{T_z A} \int \sigma_r^m p_r(\sigma_r) \delta\sigma_r \quad (1.4)$$

For a narrow banded Gaussian process, Equation (1.4) can be shown to be

$$D = \frac{(8.M_0)^{m/2}}{A} \Gamma\left(\frac{2+m}{2}\right) \quad (1.5)$$

where M_0 denotes the zeroth spectral moment of stress(i.e. the mean square stress).

However, as established in the earlier sections of this paper, VIV data from the Gulf Stream experiments shows that the vibrations are not narrow banded, as shown in Figure 10 (a). Figure 10 (b) shows a histogram of the distribution of strain data. The data is normalized by its variance and presented in the form of probability of occurrence of strain amplitude. The data is compared with a Gaussian distribution with unit variance. The good match indicates that the Miami data is Gaussian distributed. It is however broad-banded which suggests that once this data is converted to stress, the Rayleigh formulation is not appropriate to derive the stress range PDF, $p_r(\sigma_r)$. Several methods have been advocated in the literature to calculate the stress range distribution of broadband Gaussian processes. A

commonly used method has been presented by Dirlik [7]. Unlike the Rayleigh formulation which is based only on the variance of the data (zeroth spectral moment), this method also uses the first, second and fourth spectral moments in empirical relations to formulate the stress range PDF, $p_r(\sigma_r)$, for a broadband spectrum. This formulation can then be used in equation (1.4) to estimate fatigue damage.

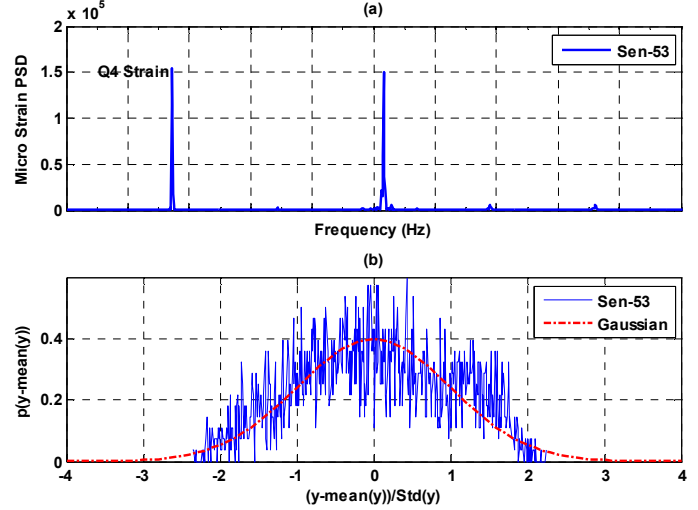


Figure 10 - The distribution of the Gulf Stream Q2 Strain data at a representative location (sensor 53 – 372.5 ft. from the top) in (a) the frequency domain (b) time domain. Also shown in (b) is a Gaussian probability distribution (mean=0, variance=1).

Figure 11 shows the comparison of stress range PDF from Rainflow counting and the Dirlik method. If we consider the Rainflow method to be accurate, it is clear that the Dirlik method predicts the shape of the stress range PDF better than the Rayleigh method. This is especially true for the low range oscillations due to the presence of the high frequencies in the data, which are totally ignored in the Rayleigh formulation.

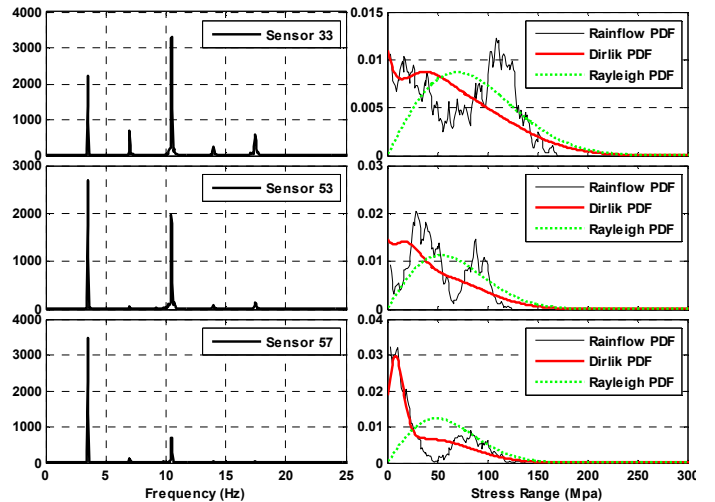


Figure 11 – Strain PSDs and corresponding stress ranges PDFs at 3 sensor locations (sensor 33 – 232.5 ft., sensor 53 – 372.5 ft., sensor 57 – 400.5 ft.).

Table 2 shows the comparisons of the fatigue calculations using the three methods. These values indicate that the Dirlik method predicts fatigue damage more accurately than the Rayleigh method.

Table 2 – The Dirlik method predicts damage more accurately than the Rayleigh method for broadband spectra.

Sensor No / Dist. Along pipe from top (ft)	Dirlik Damage / Rainflow Damage	Rayleigh Damage / Rainflow Damage
33 / 232.5	1.5014	1.7177
53 / 372.5	1.8278	2.1564
57 / 400.5	1.2467	1.4861

In summary, these results indicate that the Rayleigh method may not be appropriate for VIV fatigue predictions when the higher harmonics are present. Stress range PDFs developed for broad-band formulations are more appropriate in these situations. Since the strain, and hence stress, time series data from the second Gulf Stream which includes the higher harmonics is Gaussian distributed, the authors propose the use of the Dirlik method for estimating the stress range PDFs. Preliminary results shown above indicate better fatigue life estimates using this approach., when compared to the Rainflow counting method.

Using the Dirlik Spectrum in Design

Usually a stress time series is not available during the design phase of a VIV analysis. Therefore, including the higher harmonics in fatigue calculations involves estimating the ir magnitudes in addition to using the right formulation for estimating stress range PDFs. Having shown that the Dirlik method is more appropriate for predicting stress range PDFs when the higher harmonics are present, the authors propose a procedure below to develop the Dirlik formulation using physical insight about the higher harmonics and the 1x response from predictive programs. This procedure is referred to as the “Modified Dirlik” method in this paper

Consider a predicted stress RMS response of S_{rms} using a VIV prediction program like Shear7. It was shown earlier that this is an accurate prediction of the measured 1x RMS stress response. If f_1 is the 1x frequency, f_3 the 3x frequency and f_5 the 5x frequency, spectral moments of the total cross-flow stress spectrum can be estimated as

$$m_0 = A_1 + A_3 + A_5$$

$$m_1 = A_1 f_1 + A_3 f_3 + A_5 f_5$$

$$m_2 = A_1 f_1^2 + A_3 f_3^2 + A_5 f_5^2$$

$$m_4 = A_1 f_1^4 + A_3 f_3^4 + A_5 f_5^4$$

where A_1 , A_3 and A_5 are the areas under the stress spectrum corresponding to the 1x, 2x and 3x frequencies.

For VIV analysis, it is known that $f_3 \sim 3 * f_1$ and $f_5 \sim 5 * f_1$. Further, assuming that $A_3 = h * A_1$ and $A_5 = k * A_1$ where h and k are empirically determined factors, gives us a modified formulation for the stress spectral moments

$$m_0 = A_1 + h A_1 + k A_1 = (1 + h + k) A_1$$

$$m_1 = A_1 f_1 + (h A_1)(3 f_1) + (k A_1)(5 f_1) = (1 + 3 * h + 5 * k) A_1 f_1$$

$$m_2 = A_1 f_1^2 + (h A_1)(3 f_1)^2 + (k A_1)(5 f_1)^2 = (1 + 9 * h + 25 * k) A_1 f_1^2$$

$$m_4 = A_1 f_1^4 + (h A_1)(3 f_1)^4 + (k A_1)(5 f_1)^4 = (1 + 81 * h + 625 * k) A_1 f_1^4$$

Using $A_1 = (S_{rms})^2$, where (S_{rms}) is the RMS stress of the 1x component, gives us the final form of the above formulation as

$$m_0 = (1 + h + k) S_{rms}^2$$

$$m_1 = (1 + 3 * h + 5 * k) S_{rms}^2 f_1$$

$$m_2 = (1 + 9 * h + 25 * k) S_{rms}^2 f_1^2$$

$$m_4 = (1 + 81 * h + 625 * k) S_{rms}^2 f_1^4$$

The Dirlik stress range PDF can be developed using these spectral moments. Further, fatigue damage can be estimated using the procedure outlined earlier in the paper.

The above methodology is useful because the only unknowns in this formulation are h and k, the ratios of the spectral areas under the 3x and 5x to the spectral area under the 1x frequency. The other variables are obtained from the Strouhal number and the predicted value of RMS stress of the 1x component.

Since the strain time series was available for the Miami tests, the values of h and k can be calculated and plugged into the formulation. Using Young’s Modulus of Steel, the resulting stress range PDF compares well with the Dirlik PDFs developed using the full spectrum as shown in Figure 12. Sensor 33 (Q1 – 232.5 ft.), sensor 53 (Q4 – 372.5 ft.), sensor 57 (Q4 – 400.5 ft.) were chosen because they happened to be aligned with the cross-flow direction.

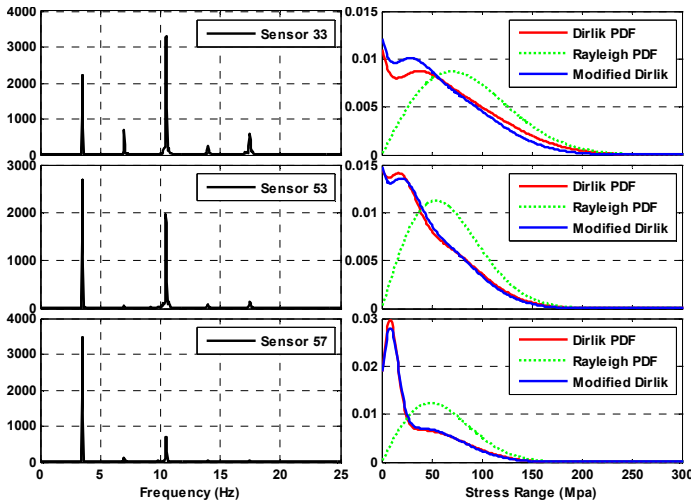


Figure 12 – Strain PSDs and corresponding stress ranges PDFs at 3 sensor locations.

Table 3 compares the fatigue damage obtained using the three methods. The results indicate that the Modified Dirlik method provides a good estimate of the fatigue caused by the higher harmonics when compared to results from the Rainflow counting method. The simplicity of the method makes it amenable to be used with predictive programs for fatigue calculations.

Table 3 – Comparison of fatigue life estimates using the Dirlik and the “Modified Dirlik” methods to those obtained using Rainflow counting analysis.

Sensor No / Dist. Along pipe from top (ft)	Dirlik Damage / Rainflow Damage	Modified Dirlik Damage / Rainflow Damage
33 / 232.5	1.5014	0.9665
53 / 372.5	1.8278	1.4874
57 / 400.5	1.2467	0.9854

Determining the values of h and k

It is clear that the determination of the ratios of spectral areas $3x/1x$ and $5x/1x$, denoted by h and k, are required before the above method can be successfully used in design. This is an area of ongoing research and some insights are becoming available.

Recent work has indicated that the ratio $3x/1x$ is dependent on the reduced velocity. Further, results from the Gulf stream experiments indicate that the third harmonic is present over a smaller reduced velocity range than the first harmonic.

Simple linear models have been developed for the $3x/1x$ and $5x/1x$ ratios using the Gulf Stream experiments. However, more data for different pipes are needed to check these models and

establish coefficients that can be used universally in predictive programs.

CONCLUSIONS

Results from the first and second Gulf Stream experiments show significant energy in the higher harmonics in certain regions of the pipe. Fatigue amplifications, when compared to fatigue damage due to just the $1x$ component in the same region, exceeding twenty were found in these regions. Therefore, the importance of incorporating the effects of the higher harmonics in fatigue damage estimates for deepwater riser is clear.

Research by the authors has found that when the field data is filtered to remove the higher harmonics, the resulting RMS strain measurements compare well with estimates from Shear7, a VIV prediction program. In some sense this is to be expected, since the predictive programs do not include the higher harmonics in their calculations. It is however encouraging to find that the predictions do match field data when compared appropriately.

Historically, the assumption that VIV is a narrow banded Gaussian process has been used to justify the use of Rayleigh methods in calculating the stress range PDF. However, significant energy at the harmonic frequencies make the stress PSD broad-banded and the Rayleigh formulation is no longer accurate. Comparisons of fatigue damage calculated using the Rayleigh formulation and Rainflow cycle counting methods indicates that the Rayleigh method overpredicts fatigue damage by 50% to 100% in most cases. The authors found that similar comparisons using the Dirlik formulation reduced fatigue estimate errors (Table 2).

Having established that the Dirlik formulation for the stress range PDF results in more accurate predictions of the fatigue damage due to VIV and that Shear7 predicts the fundamental VIV component accurately, the authors present a methodology that can include the effects of the higher harmonics in fatigue estimates. Significantly, the methodology developed uses tools and formulations currently available to engineers to expedite the implementation of the method. However, we want to draw attention to one important piece of the puzzle that still needs to be developed before the above method can be put to use. Currently, models that predict the location and magnitude of the higher harmonics are not available. Recent research [1][4] and results presented in this paper suggest that such a model will depend on, among other parameters, amplitude to diameter ratio, reduced velocity, magnitude of the current and shear in the current. Based on ongoing work by the authors and others in the research community, the authors hope such models will be available shortly.

NOMENCLATURE

- $1x, 3x \dots$ ‘x’ is interpreted as ‘times the fundamental VIV frequency of vibration’
A A material constant used in S-N curves [Stress]

A_I	Area under the peak in the stress spectrum at the Strouhal frequency [MPa^2]
E	Modulus of Elasticity of the pipe used for the second Gulf Stream experiments [MPa]
E_s	Modulus of Elasticity of Steel [$29,000 MPa$]
D	Total Fatigue Damage [$1/Yr$]
D_i	Fatigue damage caused due to the i th frequency [$1/Yr$]
m	Material Parameter that characterizes the slope of the fatigue S-N curve [-]
M_0	Zeroth moment of the strain spectra [-]
m_0, m_1, \dots	Moments of the stress spectrum
N	Number of stress cycles in time T [-]
n_r	Number of stress cycles at range σ_r in time T [-]
f	Frequency [$time^{-1}$]
$f_1, f_3 \dots$	Frequency corresponding to $1x, 3x$ etc [$time^{-1}$]
p_r	Stress Range PDF [-]
σ_r	Stress Range [MPa]
$p_a(i)$	Probability of occurrence of the i th time sharing frequency [-]
S_{rms}	RMS stress predicted using Shear7 [MPa]
T	Duration of the test [sec]
T_z	Zero-crossing period [sec]

- [7] Dirlik, T., PhD Thesis, "Application of Computers to Fatigue Analysis", Warwick University, 1985.

ACKNOWLEDGMENTS

This research was sponsored by the DEEPSTAR Consortium, the Office of Naval Research Ocean Engineering and Marine Systems program (ONR 321OE) and the SHEAR7 JIP. The authors wish to thank the crews of the NUWC Seneca Lake facility and of the R/V F. G. Walton Smith at the University of Miami Rosenstiel School of Marine and Atmospheric Science. The authors also thank Jim Chitwood from Chevron and Rob Knapp from Insensys for help and support. Finally, the authors thank their research team, including Vivek Jaiswal, Hayden Marcollo³ and Susan Swithenbank.

REFERENCES

- [1] Vandiver, J. K., Swithenbank, S. B., Jaiswal, V., Jhingran, V., "Fatigue Damage from High Mode Number Vortex Induced Vibrations" *Trans. ASME 2006 Offshore Mechanics and Arctic Engineering*, Paper No. 9240, Hamburg, June 2006
- [2] Vandiver, J.K. and Jong, J. Y., "The Relationship Between In-line and Cross-flow Vortex-induced Vibration of Cylinders", *Journal of Fluids and Structures*, **1**, pp. 381-399, 1987.
- [3] Vandiver, J.K. and Chung, T-Y., "Predicted and Measured Response of Flexible Cylinders in Sheared Flow". *Proc., ASME Winter Annual Meeting Symposium on Flow-Induced Vibration*, Chicago, December 1988.
- [4] Jauvtis, N., and Williamson, C. H. K., "The effect of two degrees of freedom on vortex-induced vibration at low mass ratio", *J. Fluid Mech.*, vol. 509, pp. 23-62, 2004
- [5] Barltrop and Adams "Dynamics of Fixed Offshore Structures", Third Edition, Butterworth & Heinemann, 1991.
- [6] DNV-RP-F204, "Riser Fatigue", 2004.

³ Dr. Marcollo now works for Amog Consulting in Melbourne, Australia